PHYSICAL REVIEW D **92,** 063510 (2015)

Primordial power spectrum features and $f_{\rm NL}$ constraints

Stefano Gariazzo,[1,2] Laura Lopez-Honorez,[3] and Olga Mena[4]

[1]*Department of Physics, University of Torino, Via P. Giuria 1, I-10125 Torino, Italy*
[2]*INFN, Sezione di Torino, Via P. Giuria 1, I–10125 Torino, Italy*
[3]*Theoretische Natuurkunde, Vrije Universiteit Brussel and The International Solvay Institutes, Pleinlaan 2, B-1050 Brussels, Belgium*
[4]*Instituto de Física Corpuscular (IFIC), CSIC-Universitat de Valencia, E-46071, Spain*

(Received 24 June 2015; published 9 September 2015)

The simplest models of inflation predict small non-Gaussianities and a featureless power spectrum. However, there exist a large number of well-motivated theoretical scenarios in which large non-Gaussianties could be generated. In general, in these scenarios the primordial power spectrum will deviate from its standard power law shape. We study, in a model-independent manner, the constraints from future large-scale structure surveys on the local non-Gaussianity parameter $f_{\rm NL}$ when the standard power law assumption for the primordial power spectrum is relaxed. If the analyses are restricted to the large-scale-dependent bias induced in the linear matter power spectrum by non-Gaussianites, the errors on the $f_{\rm NL}$ parameter could be increased by 60% when exploiting data from the future DESI survey, if dealing with only one possible dark matter tracer. In the same context, a nontrivial bias $|\delta f_{\rm NL}| \sim 2.5$ could be induced if future data are fitted to the wrong primordial power spectrum. Combining all the possible DESI objects slightly ameliorates the problem, as the forecasted errors on $f_{\rm NL}$ would be degraded by 40% when relaxing the assumptions concerning the primordial power spectrum shape. Also, the shift on the non-Gaussianity parameter is reduced in this case, $|\delta f_{\rm NL}| \sim 1.6$. The addition of cosmic microwave background priors ensures robust future $f_{\rm NL}$ bounds, as the forecasted errors obtained including these measurements are almost independent on the primordial power spectrum features, and $|\delta f_{\rm NL}| \sim 0.2$, close to the standard single-field slow-roll paradigm prediction.

DOI: 10.1103/PhysRevD.92.063510 PACS numbers: 98.80.Cq

I. INTRODUCTION

Inflationary theories have been extremely successful in explaining the horizon problem and the generation of the primordial perturbations seeding the structures of our current Universe [1–11]. The firm confirmation of these theories as the responsible ones for the Universe we observe today would come from the detection of a signal of primordial gravitational waves. A key observable to disentangle between different inflationary theories is the primordial power spectrum, i.e. the power spectrum of the initial curvature perturbations $P_{\mathcal{R}}(k)$. This power spectrum is usually taken to be a featureless primordial power spectrum (PPS), described by a simple power law $P_{\mathcal{R}}(k) \propto k^{n_s-1}$, with n_s the scalar spectral index. However, there exists a vast number of models in the literature which may give rise to a nonstandard PPS (see the recent review [12]). That is the case of slow-roll induced by phase transitions in the early universe [13–15], by some inflation potentials [16–37], by resonant particle production [38–42], variation in the sound speed of adiabatic modes [43,44] or by trans-Planckian physics [45–49]. All these nonstandard scenarios, as well as other noncanonical schemes [50–57], could lead to a PPS which may notably differ from the simple power law parametrization.

Another key observable to distinguish among the possible inflationary models is the deviation from the pure Gaussian initial conditions. Non-Gaussianities are usually described by a single parameter, $f_{\rm NL}$. In the matter-dominated universe, the gauge-invariant Bardeen potential on large scales can be parametrized as [58–61]

$$\Phi_{\rm NG} = \Phi + f_{\rm NL}(\Phi^2 - \langle\Phi^2\rangle), \tag{1}$$

where Φ is a Gaussian random field. The non-Gaussianity parameter $f_{\rm NL}$ is often considered to be a constant, yielding non-Gaussianities of the *local* type.

Traditionally, the standard observable to constrain non-Gaussianities is the cosmic microwave background (CMB), through the three-point correlation function, or bispectrum. As the odd power correlation functions vanish for the case of Gaussian random variables, the bispectrum provides the lowest-order statistic to test any departure from Gaussianity. The bispectrum is much richer than the power spectrum, as it depends on both the scale and the shape of the primordial perturbation spectra. The current bound from the complete Planck mission for the local non-Gaussianity parameter is $f_{\rm NL} = 0.8 \pm 5$ (68% C.L.) [62].

The large-scale structures of the Universe provide an independent tool to test primordial non-Gaussianites, as shown in the pioneer works of Refs. [63] and [64]. Dark matter halos will be affected by the presence of non-Gaussianties, and a scale-dependent bias will characterize

the non-Gaussian signal at large scales [65–71]. The tightest bounds on primordial non-Gaussianity using exclusively large-scale structure data are those obtained from DR8 photometric data (see Ref. [72]) which exploit 800,000 quasars and finds $-49 < f_{\rm NL} < 31$ (see also Ref. [73]). While current large-scale structure constraints are highly penalized due to their systematic uncertainties, it has been shown by a number of authors that the prospects from upcoming future large-scale structure surveys can reach $\sigma(f_{\rm NL}) < 1$ [71,74–84].

Even if Eq. (1) is commonly used in the literature assuming a scale-independent parameter $f_{\rm NL}$, let us mention that some theoretical scenarios can give rise to a scale-dependent $f_{\rm NL}$ [85–88]. This scale dependence has already been studied in several works (see e.g. [89–91]) using large-scale structure information, cluster number counts and/or CMB spectral information. The forecast on the errors on the non-Gaussianity parameters are, however, known to be parametrization/model dependent [90,91]. The recent work of Ref. [91] focuses on the complementarity of the different cosmological probes, which could help enormously to determine the functional dependence of a scale-dependent non-Gaussianity parameter without having to assume a particular choice of such a scale dependence. In particular, they make use of spectral distortions of the CMB background. In this work, we shall focus on the forecasts associated to future large-scale structure probes only and we will restrict ourselves to a scale-independent parameter $f_{\rm NL}$. However, when allowing for a nonstandard primordial power spectrum as well, additional measurements of the CMB distortion parameters could help in removing some of the degeneracies that appear between non-Gaussianities and the parameters governing the primordial power spectrum parametrization. Furthermore, these degeneracies could copiously appear in the case of scale-dependent non-Gaussianities.

Despite the fact that the simplest models of inflation (i.e. single-field, slow-rolling with a canonical kinetic term) predict small non-Gaussianities, there are some theoretical scenarios in which large non-Gaussianties could be generated; see e.g. Ref. [92] and references therein. The same deviations from the standard slow-roll inflation that give rise to non-Gaussianities could also be a potential source for other features in the PPS [15], which are absent in the simplest inflation models. Particle production during inflation gives rise to both a noncanonical PPS and large non-Gaussianities simultaneously [42]. These two phenomena could also appear together in single-field models with nonstandard inflationary potentials [20,21,24,32,34,36], as well as in brane inflation [29] and multifield inflationary models [33]. Other possibilities that will give rise to both a nonstandard matter power spectrum and non-Gaussianities include preheating scenarios [93,94].

As nature could have chosen other inflationary scenario rather than the single-field slow-roll paradigm, it is interesting to explore, in a model-independent way, how the forecasts for large-scale structure surveys concerning future measurements of $f_{\rm NL}$ are affected when the assumption of a standard PPS is relaxed. This has never been done before while forecasting errors on the $f_{\rm NL}$ parameter and it is a mandatory calculation, because models which will produce non-Gaussianities will likely give rise to a nonstandard PPS as well. Even if non-Gaussianties and distortions from the standard power law PPS are expected to be governed by the same fundamental physics, (and, therefore, related to each other), the underlying inflationary mechanism is unknown *a priori*. A conservative and general approach is, therefore, to treat these two physical effects as independent and to be determined simultaneously. This is the strategy we follow in this paper. The structure of this manuscript is as follows. We start describing the parametrization of the PSS used here in Sec. II. Section III A describes the scale-dependent halo bias in the matter power spectrum, while in Sec. III B we describe the methodology followed for our calculations as well as the specifications of the future large-scale structure survey illustrated here. We present our results in Sec. III C and conclude in Sec. IV.

II. PRIMORDIAL POWER SPECTRUM

The simplest models of inflation predict a power law form for the PPS of scalar and tensor perturbations. As previously stated, in principle, a different shape for the PPS (see Ref. [12] and references therein), can be generated by more complicated inflationary models (see e.g. Ref. [95] for some compilation). In order to explore the robustness of future forecasted errors from large-scale structure surveys on the local non-Gaussianity parameter $f_{\rm NL}$, we assume a nonparametric form for the PPS, following the prescription of Ref. [96], which is an example of a number of possible methods explored in the literature [97–125]. We describe the PPS of the scalar perturbations by means of a function to interpolate the PPS values in a series of nodes at fixed position. The function we exploit to interpolate is commonly called the "piecewise cubic Hermite interpolating polynomial," the `PCHIP` algorithm [126]; see Appendix A of Ref. [96] for details concerning the version of the `PCHIP` algorithm [127] used in the following. Within this model, one only needs to provide the values of the PPS in a discrete number of nodes and to interpolate among them. As in previous work [96], we define the PPS at twelve nodes, whose values of k are:

$$\begin{aligned} k_1 &= 5 \times 10^{-6}\ \mathrm{Mpc}^{-1}, \\ k_2 &= 10^{-3}\ \mathrm{Mpc}^{-1}, \\ k_j &= k_2 (k_{11}/k_2)^{(j-2)/9} \quad \text{for } j \in [3,10], \\ k_{11} &= 0.35\ \mathrm{Mpc}^{-1}, \\ k_{12} &= 10\ \mathrm{Mpc}^{-1}. \end{aligned} \tag{2}$$

In the range (k_2, k_{11}), that has been shown to be well constrained by current cosmological data [124], we choose equally spaced nodes (in logarithmic scale). The purpose of the first and the last nodes is to allow for a nonconstant behavior of the PPS outside the well-constrained range. The PCHIPPCHIP PPS is given by

$$P(k) = P_0 \times \texttt{PCHIP}(k; P_{s,1}, \ldots, P_{s,12}), \tag{3}$$

with $P_{s,j}$ the value of the PPS at the node k_j divided by $P_0 = 2.2 \times 10^{-9}$, according to the latest results from the Planck Collaboration; see Ref. [128].

III. FORECASTS

A. Non-Gaussian halo bias

Non-Gaussianities as introduced in Eq. (1) induce a scale-dependent bias that affects the matter power spectrum at large scales. This scale-dependent bias reads as [63,65]

$$\delta_g = b\delta_{\rm dm} \quad \text{where } b = b_G + \Delta b, \tag{4}$$

where $\delta_g(\delta_{\rm dm})$ are galaxy (dark matter) overdensities, $b_{\rm G}$ is the Gaussian bias and Δb reads as

$$\Delta b = 3 f_{\rm NL}(1 - b_G)\delta_{\rm c} \frac{H_0^2 \Omega_{\rm m}}{k^2 T(k) D(a)}, \tag{5}$$

with $T(k)$ the linear transfer function. The growth factor $D(a)$ is defined as $\delta_{\rm dm}(a)/\delta_{\rm dm}(a=1)$ and δ_c refers to the linear overdensity for spherical collapse [129]. The power spectrum with non-Gaussianties included is obtained using

$$P_{\rm ng} = P(b_G + \Delta b + f\mu_k^2)^2, \tag{6}$$

where μ_k is the cosine of the angle between the line of sight and the wave vector k and f is defined as $d\ln\delta_{\rm dm}/d\ln a$. P is the dark matter power spectrum, whose k dependence is driven either by Eq. (3) or by the standard power law matter power spectrum (with a given amplitude A_s and slope n_s).

In Fig. 1, top panel, we illustrate the galaxy power spectrum in the absence of non-Gaussianites (i.e. $f_{\rm NL} = 0$) as well as for the $f_{\rm NL} = 20$ case. We also show—see the thin red dashed line—that using a PCHIP PPS with $f_{\rm NL} = 0$ it is possible to match the galaxy power spectrum obtained with a standard power law PPS and $f_{\rm NL} \neq 0$. The $P_{s,j}$ values needed to obtain such an effect were taken to be within their currently 95% C.L. allowed regions [96]. Therefore, large degeneracies between the $P_{s,j}$ nodes and $f_{\rm NL}$ parameter are expected. Such a large value of $f_{\rm NL} = 20$, albeit allowed by the current large-scale structure limits on local non-Gaussianities, is much larger than the expected errors from the upcoming galaxy redshift surveys (see e.g. Refs. [76,130]). Therefore, we also illustrate in Fig. 1, bottom panel, the equivalent plot for

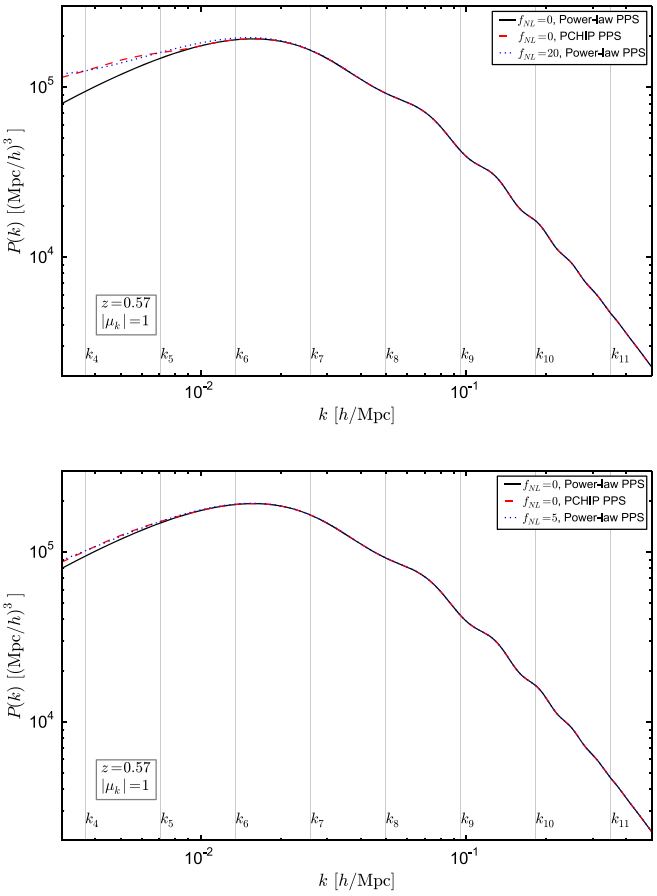

FIG. 1 (color online). The upper panel depicts the galaxy power spectrum for the standard PPS power law case, for $f_{\rm NL} = 0$ (black solid curve) and $f_{\rm NL} = 20$ (blue dotted curve), together with a PCHIP PPS case (red dashed lines) for $f_{\rm NL} = 0$. The values of the PCHIP PPS nodes are chosen accordingly to match the predictions of the $f_{\rm NL} = 20$ case. The lower panel shows the equivalent but for $f_{\rm NL} = 5$. We have also changed accordingly the value of the PCHIP PPS nodes. We also show with k_i for $i = 4, \ldots, 11$ the k position of five of the nodes considered in our analysis ($i = 5, \ldots, 9$), plus $k_{4,10,11}$ that lie outside the k range probed by the DESI experiment. The galaxy power spectra are obtained for $z = 0.57$, $|\mu_k| = 1$ and assuming a constant Gaussian bias b_G.

$f_{\rm NL} = 5$. For this case, the values for the PPS nodes $P_{s,j}$ required to match the predictions from a standard power law PPS lie within their 68% C.L. current allowed regions [96]. However, notice that the degeneracies are still present. We, therefore, expect that the forecasted errors on the $f_{\rm NL}$ parameter are largely affected by the uncertainties on the precise PPS shape.

B. Methodology

We focus here on the future spectroscopic galaxy survey DESI (Dark Energy Instrument) experiment [131]. Although multiband, full-sky imaging surveys have been shown to be the optimal setups to constrain non-Gaussianities via

large-scale structure measurements [71,74], the purpose of the current paper is to explore the degeneracies with the PPS parametrization rather than to optimize the $f_{\rm NL}$ sensitivity. Therefore, we restrict ourselves here to the DESI galaxy redshift survey (similar results could be obtained with the ESA Euclid instrument).

In order to compute the expected errors on the local non-Gaussianity parameter, we follow here the usual Fisher matrix approach, whose elements, as long as the posterior distribution for the parameters can be well approximated by a Gaussian function, read as [132–134]

$$F_{\alpha\beta} = \frac{1}{2}\mathrm{Tr}[C^{-1}C_{,\alpha}C^{-1}C_{,\beta}], \tag{7}$$

with $C = S + N$ the total covariance. The covariance matrix contains both the signal S and the noise N terms, and $C_{,\alpha}$ refer to its derivatives with respect to the cosmological parameter p_α in the context of the underlying fiducial cosmology. The 68% C.L. marginalized error on a given parameter p_α is $\sigma(p_\alpha) = \sqrt{(F^{-1})_{\alpha\alpha}}$, with F^{-1} the inverse of the Fisher matrix. In the following, in order to highlight the differences in the error on the $f_{\rm NL}$ parameter arising from different PPS choices, we only consider information concerning non-Gaussianites from large-scale structure data, neglecting the information that could be added from CMB bispectrum measurements.

Our large-scale structure Fisher matrix reads as [135]

$$\begin{aligned} F^{\rm LSS}_{\alpha\beta} &= \int_{\vec{k}_{\rm min}}^{\vec{k}_{\rm max}} \frac{\partial \ln P_{\rm ng}(\vec{k})}{\partial p_\alpha}\frac{\partial \ln P_{\rm ng}(\vec{k})}{\partial p_\beta} V_{\rm eff}(\vec{k})\frac{d\vec{k}}{2(2\pi)^3} \\ &= \int_{-1}^{1}\int_{k_{\rm min}}^{k_{\rm max}} \frac{\partial \ln P_{\rm ng}(k,\mu_k)}{\partial p_\alpha}\frac{\partial \ln P_{\rm ng}(k,\mu_k)}{\partial p_\beta} V_{\rm eff}(k,\mu_k) \\ &\quad \times \frac{2\pi k^2 dk d\mu_k}{2(2\pi)^3}, \end{aligned} \tag{8}$$

where $V_{\rm eff}$ is the effective volume of the survey,

$$V_{\rm eff}(k,\mu_k) = \left[\frac{nP_{\rm ng}(k,\mu_k)}{nP_{\rm ng}(k,\mu_k)+1}\right]^2 V_{\rm survey}, \tag{9}$$

where $P_{\rm ng}$ is the power spectrum with non-Gaussianities included [see Eq. (6)] and n refers to the galaxy number density per redshift bin. We assume $k_{\rm max} = 0.1$ h/Mpc and $k_{\rm min}$ is chosen to be equal to $2\pi/V^{1/3}$, where V represents the volume of the redshift bin. The DESI survey is expected to cover 14000 deg^2 of the sky in the redshift range $0.15 < z < 1.85$, divided in redshift bins of width $\Delta z = 0.1$. We follow Ref. [136] for the number densities $n(z)$ and biases $b_G(z)$ associated to the three types of DESI tracers: luminous red galaxies (LRGs), emission line galaxies (ELGs) and high redshift quasars (QSOs). We include the redshift dependence of the (fiducial) bias b_G in Eq. (6) as follows: $b_G(z)D(z) = 0.84, 1.7, 1.2$ for ELG, LRG and QSOs, respectively, where $D(z)$ is the growth factor as in Eq. (5). In order to combine the three different Fishers matrices from the three DESI tracers (LRGs, ELGs and QSOs), we follow the multitracer formalism developed in Ref. [137], where the authors present a generic expression for the Fisher information matrix of surveys with any number of tracers. The multitracer technique provides constraints that can surpass those set by cosmic variance, due to the differences in the clustering of the possible tracers of large-scale structure.

Also, let us remind that the observed size of an object or a feature at a given redshift z are obtained in terms of redshift and angular quantities Δz and $\Delta\theta$. These two quantities are related to the comoving dimensions $r_\parallel$ and $r_\perp$ along and across the line of sight through the angular diameter distance $D_A(z)$ and the Hubble rate $H(z)$. The same applies to the Fourier transform associated variables (we will refer to these as $k_\parallel$ and $k_\perp$ for the dual coordinates of $r_\parallel$ and $r_\perp$). Therefore, when one aims to reconstruct the measurements of galaxy redshifts and positions in some reference cosmological model which differ from a given fiducial cosmology, one has to account for geometrical effects in the following way [135],

$$P_{\rm obs}(k^{\rm ref}_\parallel, k^{\rm ref}_\perp) = \frac{D_A(z)|^2_{\rm ref}}{D_A(z)^2}\frac{H(z)}{H(z)|_{\rm ref}} P_{\rm fid}(k_\parallel, k_\perp), \tag{10}$$

where the *ref* sub/superscript denotes quantities in the reference cosmological model.[1] We properly account for such effects in our Fisher matrix forecasts when taking numerical derivatives of the galaxy power spectrum with respect to the cosmological parameters at given values of $|\mathbf{k}|$ and μ_k (or equivalently, of $k_\parallel$ and $k_\perp$).

In addition to Fisher matrix forecasts, we will also compute the expected shift in the $f_{\rm NL}$ parameter if the $P_{s,j}$ PCHIP parameters (with $j = 5, \ldots, 9$) are (incorrectly) set to values different from their fiducial ones. For that purpose, we use the method developed by the authors of Ref. [138]. The main idea is as follows: if the future DESI data are fitted assuming a cosmological model with fixed values of $P_{s,j}$[2] and, therefore, characterized by $n' = 5$ parameters $\mathcal{M}' = \{\Omega_b h^2, \Omega_c h^2, h, f_{\rm NL}, w\}$, but the true underlying cosmology is a model with different values of $P_{s,j}$ and, therefore, characterized by $n = 10$ parameters $\mathcal{M} = \{\Omega_b h^2, \Omega_c h^2, h, f_{\rm NL}, w, P_{s,j}\}$ (with $j = 5, \ldots, 9$), the inferred values of the $n' = 5$ parameters will be shifted from their true values to compensate for the fact that the model used to fit the data is wrong. Assuming that the likelihood is Gaussian, the shifts in the n' parameters read as [138]

[1] $k_\parallel = k^{\rm ref}_\parallel D_A(z)|_{\rm ref}/D_A(z)$ and $k_\perp = k^{\rm ref}_\perp H(z)/H(z)|_{\rm ref}$.

[2] Fixing the values of $P_{s,j}$ corresponds to fix both n_s and A_s to their best-fit values according to the normalization used here.

TABLE I. Marginalized 1-σ constraints on the parameters associated to the standard PPS assuming a fiducial value $f_{\rm NL} = 20$. The error on the amplitude of the power spectrum is evaluated on $A_s/(2.2 \times 10^{-9})$.

	Fiducial	LRG	ELG	QSO	All
$\Omega_b h^2$	0.02267	4.78×10^{-3}	4.86×10^{-3}	5.11×10^{-3}	2.38×10^{-3}
$\Omega_c h^2$	0.1131	1.75×10^{-2}	1.65×10^{-2}	1.51×10^{-2}	7.70×10^{-3}
h	0.705	5.02×10^{-2}	5.01×10^{-2}	4.69×10^{-2}	2.42×10^{-2}
n_s	0.96	5.68×10^{-2}	4.28×10^{-2}	4.12×10^{-2}	1.96×10^{-2}
A_s	2.2×10^{-9}	0.341	0.331	0.302	0.156
$f_{\rm NL}$	20	19.9	10.1	8.56	4.79
w	-1	5.38×10^{-2}	4.09×10^{-2}	6.18×10^{-2}	2.36×10^{-2}

$$\delta\theta'_\alpha = -(F'^{-1})_{\alpha\beta} G_{\beta\zeta} \delta\psi_\zeta \alpha, \qquad \beta = 1 \ldots n', \quad \zeta = n' + 1 \ldots n, \tag{11}$$

where F' is the Fisher matrix for the n' parameters model (with the $P_{s,j}$ fixed) and G denotes the Fisher matrix for the n parameters model (including the n' previous parameters plus the PCHIP $P_{s,j}$ parameters).

In the following, unless otherwise stated, we shall adopt the best-fit values from the complete Planck mission [128], which, in the standard power law PPS, corresponds to $A_s = 2.2 \times 10^{-9}$ and $n_s = 0.965$ at $k_{\rm pivot} = 0.05$. Within the PCHIP parametrization, the best-fit values used for the nodes considered in the numerical analyses below are $P_{s,5} = 1.07099$, $P_{s,6} = 1.04687$, $P_{s,7} = 1.02329$, $P_{s,8} = 1.00024$ and $P_{s,9} = 0.97771$. These values are obtained calculating the value of the best-fit power law power spectrum, given by Planck 2015 best-fit values for A_s and n_s as mentioned above, at the positions of the nodes k_5 to k_9. The remaining nodes are outside the k range expected to be covered by the DESI survey, given the values of $k_{\rm max}$ and $k_{\rm min}$ considered here.

C. Results

In the following, we shall present the results arising from our Fisher matrix calculations, for the two fiducial cosmologies explored here: one in which the PPS is described by its standard power law form, and a second one in which the PPS is described by the PCHIP parametrization. The parameters describing the model with a power law PPS are the baryon and cold dark matter physical energy densities, $\Omega_b h^2$ and $\Omega_c h^2$, the Hubble parameter h (with H_0, the Hubble constant, defined as 100 h km/s/Mpc), the scalar spectral index n_s, the amplitude of the PPS A_s, and the equation of state of the dark energy component w. The PCHIP PPS case is also described by $\Omega_b h^2$, $\Omega_c h^2$, h, w plus five nodes $P_{s,j}$ (with j ranging from 5 to 9) describing the PCHIP PPS. Non-Gaussianites of the local type are implemented in both fiducial cosmologies via the $f_{\rm NL}$ parameter. All the results described below (unless otherwise stated) refer to the analysis of the three DESI tracers (ELGs, LRGs and QSOs); i.e., they have been obtained exploiting exclusively the scale-dependent biases imprinted in the power spectra of these three types of tracers.

Table I (II) shows the 1σ marginalized errors for the case of a standard (PCHIP) PPS, for a fiducial value $f_{\rm NL} = 20$ for each of the DESI tracers as well as the error from the combination of all of them, using the multitracer technique. Even if such a value of the $f_{\rm NL}$ parameter ($f_{\rm NL} = 20$) is larger than the expected sensitivity from future probes, it is still allowed by current large-scale structure bounds on primordial non-Gaussianities. Notice that, for the standard power law PPS, the expected error on $f_{\rm NL}$ is 19.9, 10.1 and 8.56 for LRGs, ELGs and QSOs, respectively, while for the case of the PCHIP parametrization, one obtains $\sigma(f_{\rm NL}) =$ 32.2, 13.3 and 12.6, respectively. Therefore, there is a large increase in the error on the non-Gaussianity parameter, which can reach the 60% level. Concerning the remaining cosmological parameters, they are barely affected. In some cases, their error is even smaller than in the standard power law scenario. This is indeed the case of the equation of state parameter w, or $\Omega_b h^2$ and $\Omega_c h^2$ (the errors on the latter two parameters are smaller than in the standard PPS approach only when exploiting either ELGs or QSOs tracers). The combination of the data from the three tracers exploiting the multitracer technique alleviates the problem with the error on $f_{\rm NL}$, as the increase in the value of $\sigma(f_{\rm NL})$ when relaxing the assumption of a simple power law PPS is around 40%, rather than 60%.

The reason for this generic increase in the error of $f_{\rm NL}$ is due to the large degeneracies between the non-Gaussianity $f_{\rm NL}$ parameter and the $P_{s,j}$ nodes, which get reduced when combining the tracers. The top and bottom panels of Fig. 2 illustrate the large degeneracies between the non-Gaussianity $f_{\rm NL}$ parameter, for the fiducial value $f_{\rm NL} = 20$ and two of the $P_{s,j}$ nodes, $P_{s,5}$ and $P_{s,9}$. We only show here these two nodes, but similar degeneracies are obtained for the remaining nodes.

This degeneracy problem could *a priori* be solved in two ways, either exploiting smaller scales in the observed galaxy or quasar power spectra, or using CMB priors. In practice, going to the mildly nonlinear regime would require new additional $P_{s,j}$ nodes and new degeneracies between these additional $P_{s,j}$ nodes and the non-Gaussianity parameter $f_{\rm NL}$ will appear. We have

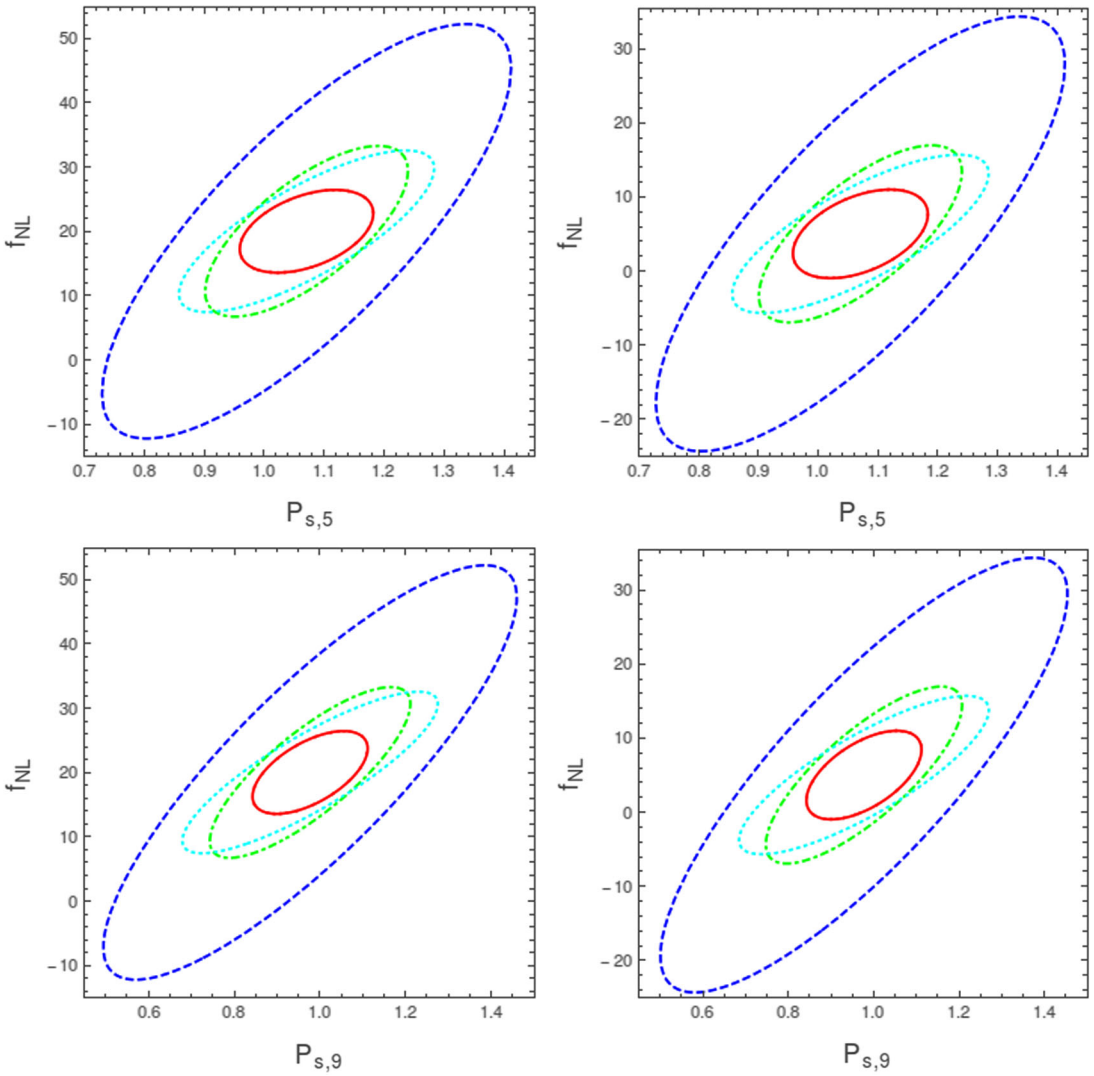

FIG. 2 (color online). The upper left (right) panel shows the $f_{\rm NL} - P_{s,5}$ degeneracy, for a fiducial cosmology with $f_{\rm NL} = 20$ ($f_{\rm NL} = 5$), assuming $k_{\rm max} = 0.1$ h/Mpc. We show the 1-σ marginalized contours associated to the LRGs (in dashed blue lines), ELGs (in dot-dashed green lines), QSOs (in dotted cyan lines) and multitracer (in solid red) Fisher matrix analyses. The bottom panels shows the analogous but in the $(f_{\rm NL} - P_{s,9})$ plane.

numerically checked that such a possibility does indeed not solve the problem. Furthermore, a nonlinear description of the matter power spectrum will depend on additional parameters, enlarging the number of degeneracies. In contrast, the CMB priors on both the PPS parameters as well as on the dark matter and baryon mass-energy densities help enormously in solving the problem of the large degeneracies between the PPS parametrization and non-Gaussianities. Tables III and IV show the equivalent of I and II but including CMB priors from the Planck mission 2013 data [139]. Notice that the impact of the Planck priors is largely more significant in the PCHIP parametrization case: the $f_{\rm NL}$ errors arising from the three different dark matter tracers when the CMB information is included are smaller in the PCHIP PSS description than in the standard power law PSS modeling. When the multitracer technique is applied, the overall errors after considering Planck 2013 CMB constraints are very similar regardless on the PPS description and close to $\sigma(f_{\rm NL}) \simeq 5$.

Table V (VI) shows the 1σ marginalized errors for the case of a standard (PCHIP) PPS, for another possible non-Gaussianity parameter fiducial value, $f_{\rm NL} = 5$, from each of the DESI tracers, as well as the error arising from the combination of all of them using the multitracer technique. As in the case of $f_{\rm NL} = 20$, the error on the non-Gaussianity parameter is increased, reaching in some cases a 60% increment. The results are very similar to those obtained and illustrated before for larger non-Gaussianites. The errors on the other cosmological parameters remain unaffected under the choice of the PPS parametrization. The dark energy equation of state parameter is extracted with a smaller error in the PCHIP PPS case, and also $\Omega_b h^2$

TABLE II. Marginalized 1-σ constraints on the parameters associated to the nonstandard PPS assuming $f_{\rm NL} = 20$.

	Fiducial	LRG	ELG	QSO	All
$\Omega_b h^2$	0.02267	7.85×10^{-3}	3.65×10^{-3}	4.70×10^{-3}	2.30×10^{-3}
$\Omega_c h^2$	0.1131	2.30×10^{-2}	1.11×10^{-2}	1.41×10^{-2}	6.36×10^{-3}
h	0.705	7.67×10^{-2}	3.59×10^{-2}	4.62×10^{-2}	2.12×10^{-2}
$P_{s,5}$	1.07099	0.340	0.169	0.212	0.111
$P_{s,6}$	1.04687	0.419	0.198	0.254	0.119
$P_{s,7}$	1.02329	0.451	0.216	0.276	0.125
$P_{s,8}$	1.00024	0.479	0.229	0.293	0.132
$P_{s,9}$	0.97771	0.482	0.234	0.298	0.134
$f_{\rm NL}$	20	32.2	13.3	12.6	6.43
w	−1	4.03×10^{-2}	2.80×10^{-2}	4.45×10^{-2}	2.45×10^{-2}

TABLE III. As in Table I but including CMB priors; see the text for details.

	Fiducial	LRG	ELG	QSO	All
$\Omega_b h^2$	0.02267	2.67×10^{-4}	2.63×10^{-4}	2.66×10^{-4}	2.59×10^{-4}
$\Omega_c h^2$	0.1131	1.64×10^{-3}	1.44×10^{-3}	1.52×10^{-3}	1.24×10^{-3}
h	0.705	6.66×10^{-3}	5.24×10^{-3}	5.86×10^{-3}	4.12×10^{-3}
n_s	0.96	6.72×10^{-2}	6.41×10^{-2}	6.53×10^{-2}	5.84×10^{-3}
A_s	2.2×10^{-9}	3.87×10^{-2}	3.28×10^{-2}	3.51×10^{-2}	2.71×10^{-2}
$f_{\rm NL}$	20	17.4	9.14	7.58	4.56
w	−1	4.51×10^{-2}	3.36×10^{-2}	5.44×10^{-2}	2.17×10^{-2}

TABLE IV. As in Table II but including CMB priors.

	Fiducial	LRG	ELG	QSO	All
$\Omega_b h^2$	0.02267	3.92×10^{-4}	3.79×10^{-4}	3.87×10^{-4}	3.74×10^{-4}
$\Omega_c h^2$	0.1131	1.36×10^{-3}	1.10×10^{-3}	1.18×10^{-3}	1.04×10^{-3}
h	0.705	4.13×10^{-3}	3.14×10^{-3}	3.62×10^{-3}	2.93×10^{-3}
$P_{s,5}$	1.07099	2.98×10^{-2}	2.69×10^{-2}	2.77×10^{-2}	2.60×10^{-2}
$P_{s,6}$	1.04687	2.89×10^{-2}	2.10×10^{-2}	2.32×10^{-2}	1.99×10^{-2}
$P_{s,7}$	1.02329	2.00×10^{-2}	1.73×10^{-2}	1.84×10^{-2}	1.69×10^{-2}
$P_{s,8}$	1.00024	1.92×10^{-2}	1.76×10^{-2}	1.86×10^{-2}	1.73×10^{-2}
$P_{s,9}$	0.97771	2.59×10^{-2}	2.31×10^{-2}	2.42×10^{-2}	2.22×10^{-2}
$f_{\rm NL}$	20	13.0	6.85	5.64	4.75
w	−1	3.24×10^{-2}	2.46×10^{-2}	4.0×10^{-2}	2.28×10^{-2}

and $\Omega_c h^2$ are determined with a smaller error in that case while dealing with either ELGs or QSOs tracers. The multitracer technique provides a reduction on the $f_{\rm NL}$ error similar to that obtained in the $f_{\rm NL} = 20$ case. The top and bottom right panels of Fig. 2 illustrate the large degeneracies between the non-Gaussianity $f_{\rm NL}$ parameter and two of the $P_{s,j}$ nodes, $P_{s,5}$ and $P_{s,9}$ for the fiducial value $f_{\rm NL} = 5$. Notice that the degeneracy pattern appears to be independent of the value of $f_{\rm NL}$. The addition of the CMB priors brings the errors on all the cosmological parameters ($f_{\rm NL}$ included) to the same values in both PPS parametrizations (standard power law and PCHIP PPS prescriptions), as shown in Tables VII and VIII.

We now perform an additional forecast. We focus here on the shift induced in the local non-Gaussianity parameter $f_{\rm NL}$, which we set to zero in the two cosmologies $\mathcal{M}$ and $\mathcal{M}'$. For the purpose of this analysis, we fix all of the $P_{s,j}$ to their best-fit values according to the Planck 2013 results, for the case of the $\mathcal{M}'$ cosmology. A shift in $f_{\rm NL}$ is expected to compensate for the fact that the $P_{s,j}$ PCHIP nodes are additional parameters in $\mathcal{M}$, while not being considered as free parameters in the $\mathcal{M}'$ analysis. Therefore, we displace the $P_{s,j}$ parameters (with $j = 5, \ldots, 9$) from their fixed fiducial values in $\mathcal{M}'$; i.e., we are adding them as additional parameters in the cosmological model (i.e. to be determined by data).

TABLE V. Marginalized 1-σ constraints on the parameters associated to the standard PPS assuming a fiducial value $f_{\rm NL} = 5$. The error on the amplitude of the power spectrum is evaluated on $A_s/(2.2 \times 10^{-9})$.

	Fiducial	LRG	ELG	QSO	All
$\Omega_b h^2$	0.02267	4.78×10^{-3}	5.17×10^{-3}	5.18×10^{-3}	2.45×10^{-3}
$\Omega_c h^2$	0.1131	1.73×10^{-2}	1.73×10^{-2}	1.52×10^{-2}	7.88×10^{-3}
h	0.705	5.0×10^{-2}	5.29×10^{-2}	4.75×10^{-2}	2.48×10^{-2}
n_s	0.96	5.59×10^{-2}	4.40×10^{-2}	4.11×10^{-2}	2.0×10^{-2}
A_s	2.2×10^{-9}	0.339	0.347	0.305	0.160
$f_{\rm NL}$	5	18.9	9.32	7.83	4.45
w	-1	5.38×10^{-2}	4.13×10^{-2}	6.19×10^{-2}	2.38×10^{-2}

TABLE VI. As in Table VI, but including CMB priors.

	Fiducial	LRG	ELG	QSO	All
$\Omega_b h^2$	0.02267	3.92×10^{-4}	3.79×10^{-4}	3.86×10^{-4}	3.75×10^{-4}
$\Omega_c h^2$	0.1131	1.36×10^{-3}	1.10×10^{-3}	1.18×10^{-3}	1.04×10^{-3}
h	0.705	4.10×10^{-3}	3.13×10^{-3}	3.59×10^{-3}	2.92×10^{-3}
$P_{s,5}$	1.07099	2.98×10^{-2}	2.68×10^{-2}	2.77×10^{-2}	2.60×10^{-2}
$P_{s,6}$	1.04687	2.89×10^{-2}	2.11×10^{-2}	2.33×10^{-2}	2.0×10^{-2}
$P_{s,7}$	1.02329	2.00×10^{-2}	1.73×10^{-2}	1.84×10^{-2}	1.69×10^{-2}
$P_{s,8}$	1.00024	1.92×10^{-2}	1.76×10^{-2}	1.86×10^{-2}	1.73×10^{-2}
$P_{s,9}$	0.97771	2.50×10^{-2}	2.31×10^{-2}	2.43×10^{-2}	2.22×10^{-2}
$f_{\rm NL}$	5	12.4	6.42	5.23	4.46
w	-1	3.23×10^{-2}	2.46×10^{-2}	3.99×10^{-2}	2.27×10^{-2}

TABLE VII. As in Table V but including CMB priors; see the text for details.

	Fiducial	LRG	ELG	QSO	All
$\Omega_b h^2$	0.02267	2.67×10^{-4}	2.63×10^{-4}	2.67×10^{-4}	2.59×10^{-4}
$\Omega_c h^2$	0.1131	1.64×10^{-3}	1.43×10^{-3}	1.52×10^{-3}	1.24×10^{-3}
h	0.705	6.66×10^{-3}	5.23×10^{-3}	5.85×10^{-3}	4.11×10^{-3}
n_s	0.96	6.71×10^{-3}	6.40×10^{-3}	6.53×10^{-3}	5.84×10^{-3}
A_s	2.2×10^{-9}	3.87×10^{-2}	3.27×10^{-2}	3.51×10^{-2}	2.70×10^{-2}
$f_{\rm NL}$	5	16.8	8.56	7.12	4.27
w	-1	4.50×10^{-2}	3.36×10^{-2}	5.43×10^{-2}	2.17×10^{-2}

TABLE VIII. Marginalized 1-σ constraints on the parameters associated to the nonstandard PPS assuming $f_{\rm NL} = 5$.

	Fiducial	LRG	ELG	QSO	All
$\Omega_b h^2$	0.02267	7.72×10^{-3}	3.61×10^{-3}	4.61×10^{-3}	2.31×10^{-3}
$\Omega_c h^2$	0.1131	2.28×10^{-2}	1.09×10^{-2}	1.38×10^{-2}	6.37×10^{-3}
h	0.705	7.56×10^{-2}	3.54×10^{-2}	4.52×10^{-2}	2.13×10^{-2}
$P_{s,5}$	1.07099	0.342	0.169	0.215	0.113
$P_{s,6}$	1.04687	0.415	0.196	0.251	0.120
$P_{s,7}$	1.02329	0.445	0.212	0.270	0.126
$P_{s,8}$	1.00024	0.472	0.225	0.287	0.133
$P_{s,9}$	0.97771	0.476	0.230	0.292	0.135
$f_{\rm NL}$	5	29.3	11.9	10.7	5.97
w	-1	4.02×10^{-2}	2.79×10^{-2}	4.45×10^{-2}	2.44×10^{-2}

Referring to the notations of Eq. (11), using a shift $\delta\psi_{P_{s,j}} = 0.1$, which is smaller than the 1σ expected errors (see Tables II and VI), we obtain that the corresponding shift in the $f_{\rm NL}$ parameter is $\delta\theta_{f_{\rm NL}} \simeq 2.5$, regardless of the exploited dark matter tracer. This is a quite large displacement of the local non-Gaussianity parameter which will induce a non-negligible bias in reconstructing the inflationary mechanism. While the remaining cosmological parameters are also slightly displaced with respect to their fiducial values, their shifts will not induce a misinterpretation of the underlying true cosmology. The non-Gaussianity shift $\delta\theta_{f_{\rm NL}}$ could be a potential problem when extracting the (true) value of the $f_{\rm NL}$ parameter not only for the DESI survey, but also for future experiments with improved sensitivities to non-Gaussianities, such as SPHEREx [75]. The combination of all the three possible DESI tracers leads to a smaller shift in the $f_{\rm NL}$ parameter ($\delta\theta_{f_{\rm NL}} \simeq 1.6$). If CMB priors are applied, the shift is considerably reduced, $\delta\theta_{f_{\rm NL}} \simeq 0.2$, which is close to the expectations for non-Gaussianities in the most economical inflationary models, i.e. within single-field slow-roll inflation [92,140].

IV. CONCLUSIONS

While the simplest inflationary picture describes the power spectrum of the initial curvature perturbations $P_{\mathcal{R}}(k)$ by a simple power law without features, there exists a large number of well-motivated inflation models that could give rise to a nonstandard PPS. The majority of these models will also generate non-Gaussianities. The large-scale structure of the Universe provides, together with the CMB bispectrum, a tool to test primordial non-Gaussianites. Plenty of work has been devoted in the literature to forecast the expectations from upcoming galaxy surveys, such as the Dark Energy Instrument (DESI) experiment. The forecasted errors and bounds on the non-Gaussianity local parameter $f_{\rm NL}$ are, however, usually derived under the assumption of a standard power law PPS. Here we relax such an assumption and compute the expected sensitivity to $f_{\rm NL}$ from the DESI experiment assuming that both the precise shape of the primordial power spectrum and the non-Gaussianity parameter need to be extracted simultaneously. If the analysis is restricted to large-scale structure data, the standard errors computed assuming a featureless power spectrum are enlarged by 60% within the PCHIP PPS parametrization explored here and when treating each of the possible dark matter tracers individually. Another potential problem in future galaxy surveys could be induced by the (wrong) assumption of a featureless PSS (while nature could have chosen a more complicated inflationary mechanism leading to a nontrivial PPS). If future data are fitted to the wrong PPS cosmology, a shift in $|\delta\theta_{f_{\rm NL}}| \simeq 2.5$ would be inferred (for $k_{\rm max} = 0.1$ h/Mpc) even if the true cosmology has $f_{\rm NL} = 0$. The multitracer technique helps in alleviating the former two problems. After combining all the DESI possible tracers, the forecasted errors on $f_{\rm NL}$ will be degraded by 40% (when compared to the value obtained within the standard power law PPS model) and the resulting shift will be reduced to $|\delta\theta_{f_{\rm NL}}| \simeq 1.6$. The addition of cosmic microwave background priors from the Planck 2013 data on the PPS parameters and on the dark matter and baryon mass-energy densities leads to a $f_{\rm NL}$ error which is independent of the PPS parametrization used in the analysis. After considering CMB priors, the value of the shift $|\delta\theta_{f_{\rm NL}}|$ is 0.2, which is of the order of standard predictions for single-field slow-roll inflation [92,140].

ACKNOWLEDGMENTS

The authors would like to thank Roland de Putter for very useful comments on the manuscript. This work was supported by the European Union Program FP7 ITN INVISIBLES (Marie Curie Actions, PITN-GA-2011-289442). O. M. is supported by Program PROMETEO II/2014/050, by the Spanish Grant No. FPA2011–29678 and by the Centro de Excelencia Severo Ochoa Program, under Grant No. SEV-2014-0398, of the Spanish MINECO. L. L. H. was supported in part by FWO-Vlaanderen with the postdoctoral fellowship Project No. 1271513 and the Project No. G020714N, by the Belgian Federal Science Policy Office through the Interuniversity Attraction Pole P7/37 and by the Vrije Universiteit Brussel through the Strategic Research Program High-Energy Physics. The work of S. G. was supported by the Theoretical Astroparticle Physics research Grant No. 2012CPPYP7 under the Program PRIN 2012 funded by the Ministero dell'Istruzione, Università e della Ricerca (MIUR).

[1] A. H. Guth, Phys. Rev. D **23**, 347 (1981).
[2] A. D. Linde, Phys. Lett. **108B**, 389 (1982).
[3] A. A. Starobinsky, Phys. Lett. **117B**, 175 (1982).
[4] S. W. Hawking, Phys. Lett. **115B**, 295 (1982).
[5] A. Albrecht and P. J. Steinhardt, Phys. Rev. Lett. **48**, 1220 (1982).
[6] V. F. Mukhanov, H. A. Feldman, and R. H. Brandenberger, Phys. Rep. **215**, 203 (1992).

[7] V. F. Mukhanov and G. V. Chibisov, Pis'ma Zh. Eksp. Teor. Fiz. **33**, 549 (1981) [JETP Lett. **33**, 532 (1981)].
[8] F. Lucchin and S. Matarrese, Phys. Rev. D **32**, 1316 (1985).
[9] D. H. Lyth and A. Riotto, Phys. Rep. **314**, 1 (1999).
[10] B. A. Bassett, S. Tsujikawa, and D. Wands, Rev. Mod. Phys. **78**, 537 (2006).
[11] D. Baumann and H. V. Peiris, Adv. Sci. Lett. **2**, 105 (2009).
[12] J. Chluba, J. Hamann, and S. P. Patil, Int. J. Mod. Phys. D **24**, 1530023 (2015).
[13] J. A. Adams, G. G. Ross, and S. Sarkar, Nucl. Phys. **B503**, 405 (1997).
[14] P. Hunt and S. Sarkar, Phys. Rev. D **70**, 103518 (2004).
[15] S. Hotchkiss and S. Sarkar, J. Cosmol. Astropart. Phys. 05 (2010) 024.
[16] A. A. Starobinsky, Pis'ma Zh. Eksp. Teor. Fiz. **55**, 477 (1992) [JETP Lett. **55**, 489 (1992)].
[17] S. M. Leach, M. Sasaki, D. Wands, and A. R. Liddle, Phys. Rev. D **64**, 023512 (2001).
[18] J. O. Gong, J. Cosmol. Astropart. Phys. 07 (2005) 015.
[19] J. A. Adams, B. Cresswell, and R. Easther, Phys. Rev. D **64**, 123514 (2001).
[20] X. Chen, R. Easther, and E. A. Lim, J. Cosmol. Astropart. Phys. 06 (2007) 023.
[21] X. Chen, R. Easther, and E. A. Lim, J. Cosmol. Astropart. Phys. 04 (2008) 010.
[22] R. N. Lerner and J. McDonald, Phys. Rev. D **79**, 023511 (2009).
[23] C. Dvorkin and W. Hu, Phys. Rev. D **81**, 023518 (2010).
[24] P. Adshead, C. Dvorkin, W. Hu, and E. A. Lim, Phys. Rev. D **85**, 023531 (2012).
[25] H. M. Hodges, G. R. Blumenthal, L. A. Kofman, and J. R. Primack, Nucl. Phys. **B335**, 197 (1990).
[26] S. M. Leach and A. R. Liddle, Phys. Rev. D **63**, 043508 (2001).
[27] M. Joy, V. Sahni, and A. A. Starobinsky, Phys. Rev. D **77**, 023514 (2008).
[28] R. K. Jain, P. Chingangbam, and L. Sriramkumar, J. Cosmol. Astropart. Phys. 10 (2007) 003.
[29] R. Bean, X. Chen, G. Hailu, S.-H. H. Tye, and J. Xu, J. Cosmol. Astropart. Phys. 03 (2008) 026.
[30] A. Ashoorioon and A. Krause, arXiv:hep-th/0607001.
[31] A. Ashoorioon, A. Krause, and K. Turzynski, J. Cosmol. Astropart. Phys. 02 (2009) 014.
[32] R. Saito, J. Yokoyama, and R. Nagata, J. Cosmol. Astropart. Phys. 06 (2008) 024.
[33] A. Achucarro, J. O. Gong, S. Hardeman, G. A. Palma, and S. P. Patil, J. Cosmol. Astropart. Phys. 01 (2011) 030.
[34] G. Goswami and T. Souradeep, Phys. Rev. D **83**, 023526 (2011).
[35] P. Brax and E. Cluzel, J. Cosmol. Astropart. Phys. 04 (2011) 014.
[36] F. Arroja, A. E. Romano, and M. Sasaki, Phys. Rev. D **84**, 123503 (2011).
[37] J. Liu and Y. S. Piao, Phys. Lett. B **705**, 1 (2011).
[38] D. J. H. Chung, E. W. Kolb, A. Riotto, and I. I. Tkachev, Phys. Rev. D **62**, 043508 (2000).
[39] G. J. Mathews, D. J. H. Chung, K. Ichiki, T. Kajino, and M. Orito, Phys. Rev. D **70**, 083505 (2004).
[40] A. E. Romano and M. Sasaki, Phys. Rev. D **78**, 103522 (2008).
[41] N. Barnaby, Z. Huang, L. Kofman, and D. Pogosyan, Phys. Rev. D **80**, 043501 (2009).
[42] N. Barnaby, Adv. Astron. **2010**, 156180 (2010).
[43] A. Achúcarro, J.-O. Gong, G. A. Palma, and S. P. Patil, Phys. Rev. D **87**, 121301 (2013).
[44] G. A. Palma, J. Cosmol. Astropart. Phys. 04 (2015) 035.
[45] R. H. Brandenberger and J. Martin, Mod. Phys. Lett. A **16**, 999 (2001).
[46] U. H. Danielsson, Phys. Rev. D **66**, 023511 (2002).
[47] K. Schalm, G. Shiu, and J. P. van der Schaar, AIP Conf. Proc. **743**, 362 (2005).
[48] P. Chen, E. D. Bloom, G. Madejski, and V. Petrosian, *Proceedings of the 22nd Texas Symposium on Relativistic Astrophysics* (Stanford, 2004).
[49] R. Easther, W. H. Kinney, and H. Peiris, J. Cosmol. Astropart. Phys. 08 (2005) 001.
[50] C. P. Burgess, J. M. Cline, F. Lemieux, and R. Holman, J. High Energy Phys. 02 (2003) 048.
[51] Y. S. Piao, B. Feng, and X. m. Zhang, Phys. Rev. D **69**, 103520 (2004).
[52] B. A. Powell and W. H. Kinney, Phys. Rev. D **76**, 063512 (2007).
[53] G. Nicholson and C. R. Contaldi, J. Cosmol. Astropart. Phys. 01 (2008) 002.
[54] A. Lasenby and C. Doran, Phys. Rev. D **71**, 063502 (2005).
[55] R. H. Ribeiro, J. Cosmol. Astropart. Phys. 5 (2012) 037.
[56] G. Dvali and S. Kachru, arXiv:hep-ph/0310244.
[57] D. Langlois and F. Vernizzi, J. Cosmol. Astropart. Phys. 01 (2005) 002.
[58] D. S. Salopek and J. R. Bond, Phys. Rev. D **42**, 3936 (1990).
[59] A. Gangui, F. Lucchin, S. Matarrese, and S. Mollerach, Astrophys. J. **430**, 447 (1994).
[60] L. Verde, L. M. Wang, A. Heavens, and M. Kamionkowski, Mon. Not. R. Astron. Soc. **313**, L141 (2000).
[61] E. Komatsu and D. N. Spergel, Phys. Rev. D **63**, 063002 (2001).
[62] P. A. R. Ade *et al.* (Planck Collaboration), arXiv: 1502.01592.
[63] N. Dalal, O. Dore, D. Huterer, and A. Shirokov, Phys. Rev. D **77**, 123514 (2008).
[64] S. Matarrese and L. Verde, Astrophys. J. **677**, L77 (2008).
[65] A. Slosar, C. Hirata, U. Seljak, S. Ho, and N. Padmanabhan, J. Cosmol. Astropart. Phys. 08 (2008) 031.
[66] N. Afshordi and A. J. Tolley, Phys. Rev. D **78**, 123507 (2008).
[67] C. Carbone, L. Verde, and S. Matarrese, Astrophys. J. **684**, L1 (2008).
[68] M. Grossi, L. Verde, C. Carbone, K. Dolag, E. Branchini, F. Iannuzzi, S. Matarrese, and L. Moscardini, Mon. Not. R. Astron. Soc. **398**, 321 (2009).
[69] V. Desjacques, U. Seljak, and I. Iliev, Mon. Not. R. Astron. Soc. **396**, 85 (2009).
[70] A. Pillepich, C. Porciani, and O. Hahn, Mon. Not. R. Astron. Soc. **402**, 191 (2010).

[71] M. Alvarez, T. Baldauf, J. R. Bond, N. Dalal, R. de Putter, O. Dor, D. Green, and C. Hirata *et al.*, arXiv:1412.4671.
[72] B. Leistedt, H. V. Peiris, and N. Roth, Phys. Rev. Lett. **113**, 221301 (2014).
[73] N. Agarwal, S. Ho, and S. Shandera, J. Cosmol. Astropart. Phys. 02 (2014) 038.
[74] R. de Putter and O. Dor, arXiv:1412.3854.
[75] O. Dor, J. Bock, P. Capak, R. de Putter, T. Eifler, C. Hirata, P. Korngut, and E. Krause *et al.*, arXiv:1412.4872.
[76] J. Byun and R. Bean, J. Cosmol. Astropart. Phys. 03 (2015) 019.
[77] A. Raccanelli, O. Dore, and N. Dalal, arXiv:1409.1927.
[78] D. Yamauchi, K. Takahashi, and M. Oguri, Phys. Rev. D **90**, 083520 (2014).
[79] S. Camera, M. G. Santos, and R. Maartens, Mon. Not. R. Astron. Soc. **448**, 1035 (2015).
[80] L. D. Ferramacho, M. G. Santos, M. J. Jarvis, and S. Camera, Mon. Not. R. Astron. Soc. **442**, 2511 (2014).
[81] S. Ferraro and K. M. Smith, Phys. Rev. D **91**, 043506 (2015).
[82] C. Fedeli, C. Carbone, L. Moscardini, and A. Cimatti, Mon. Not. R. Astron. Soc. **414**, 1545 (2011).
[83] C. Carbone, O. Mena, and L. Verde, J. Cosmol. Astropart. Phys. 07 (2010) 020.
[84] T. Giannantonio, C. Porciani, J. Carron, A. Amara, and A. Pillepich, Mon. Not. R. Astron. Soc. **422**, 2854 (2012).
[85] K. Enqvist and S. Nurmi, J. Cosmol. Astropart. Phys. 10 (2005) 013.
[86] C. T. Byrnes, M. Gerstenlauer, S. Nurmi, G. Tasinato, and D. Wands, J. Cosmol. Astropart. Phys. 10 (2010) 004.
[87] A. Riotto and M. S. Sloth, Phys. Rev. D **83**, 041301 (2011).
[88] C. T. Byrnes, K. Enqvist, S. Nurmi, and T. Takahashi, J. Cosmol. Astropart. Phys. 11 (2011) 011.
[89] M. LoVerde, A. Miller, S. Shandera, and L. Verde, J. Cosmol. Astropart. Phys. 04 (2008) 014.
[90] M. Biagetti, H. Perrier, A. Riotto, and V. Desjacques, Phys. Rev. D **87**, 063521 (2013).
[91] R. Emami, E. Dimastrogiovanni, J. Chluba, and M. Kamionkowski, Phys. Rev. D **91**, 123531 (2015).
[92] N. Bartolo, E. Komatsu, S. Matarrese, and A. Riotto, Phys. Rep. **402**, 103 (2004).
[93] A. Chambers and A. Rajantie, Phys. Rev. Lett. **100**, 041302 (2008); **101**, 149903 (2008).
[94] J. R. Bond, A. V. Frolov, Z. Huang, and L. Kofman, Phys. Rev. Lett. **103**, 071301 (2009).
[95] J. Martin, C. Ringeval, and V. Vennin, Phys. Dark Univ. **5–6**, 75 (2014).
[96] S. Gariazzo, C. Giunti, and M. Laveder, J. Cosmol. Astropart. Phys. 04 (2015) 023.
[97] P. Hunt and S. Sarkar, J. Cosmol. Astropart. Phys. 01 (2014) 025.
[98] D. K. Hazra, A. Shafieloo, and T. Souradeep, J. Cosmol. Astropart. Phys. 11 (2014) 011.
[99] P. Mukherjee and Y. Wang, Astrophys. J. **593**, 38 (2003).
[100] A. Shafieloo, T. Souradeep, P. Manimaran, P. K. Panigrahi, and R. Rangarajan, Phys. Rev. D **75**, 123502 (2007).
[101] S. M. Leach, Mon. Not. R. Astron. Soc. **372**, 646 (2006).
[102] Y. Wang, D. N. Spergel, and M. A. Strauss, Astrophys. J. **510**, 20 (1999).
[103] S. L. Bridle, A. M. Lewis, J. Weller, and G. Efstathiou, Mon. Not. R. Astron. Soc. **342**, L72 (2003).
[104] S. Hannestad, J. Cosmol. Astropart. Phys. 04 (2004) 002.
[105] M. Bridges, F. Feroz, M. P. Hobson, and A. N. Lasenby, Mon. Not. R. Astron. Soc. **400**, 1075 (2009).
[106] L. Verde and H. V. Peiris, J. Cosmol. Astropart. Phys. 07 (2008) 009.
[107] K. Ichiki and R. Nagata, Phys. Rev. D **80**, 083002 (2009).
[108] B. Hu, J. W. Hu, Z. K. Guo, and R. G. Cai, Phys. Rev. D **90**, 023544 (2014).
[109] J. A. Vázquez, M. Bridges, M. P. Hobson, and A. N. Lasenby, J. Cosmol. Astropart. Phys. 06 (2012) 006.
[110] D. K. Hazra, A. Shafieloo, and G. F. Smoot, J. Cosmol. Astropart. Phys. 12 (2013) 035.
[111] G. Aslanyan, L. C. Price, K. N. Abazajian, and R. Easther, J. Cosmol. Astropart. Phys. 08 (2014) 052.
[112] M. Matsumiya, M. Sasaki, and J. Yokoyama, J. Cosmol. Astropart. Phys. 02 (2003) 003.
[113] N. Kogo, M. Matsumiya, M. Sasaki, and J. Yokoyama, Astrophys. J. **607**, 32 (2004).
[114] A. Shafieloo and T. Souradeep, Phys. Rev. D **70**, 043523 (2004).
[115] D. Tocchini-Valentini, M. Douspis, and J. Silk, Mon. Not. R. Astron. Soc. **359**, 31 (2005).
[116] R. Nagata and J. Yokoyama, Phys. Rev. D **78**, 123002 (2008).
[117] P. Paykari, F. Lanusse, J.-L. Starck, F. Sureau, and J. Bobin, Astron. Astrophys. **566**, A77 (2014).
[118] N. Kogo, M. Sasaki, and J. Yokoyama, Phys. Rev. D **70**, 103001 (2004).
[119] G. Nicholson and C. R. Contaldi, J. Cosmol. Astropart. Phys. 07 (2009) 011.
[120] G. Nicholson, C. R. Contaldi, and P. Paykari, J. Cosmol. Astropart. Phys. 01 (2010) 016.
[121] J. Hamann, A. Shafieloo, and T. Souradeep, J. Cosmol. Astropart. Phys. 04 (2010) 010.
[122] C. Gauthier and M. Bucher, J. Cosmol. Astropart. Phys. 10 (2012) 050.
[123] D. K. Hazra, A. Shafieloo, and T. Souradeep, Phys. Rev. D **87**, 123528 (2013).
[124] R. de Putter, E. V. Linder, and A. Mishra, Phys. Rev. D **89**, 103502 (2014).
[125] A. Iqbal, J. Prasad, T. Souradeep, and M. A. Malik, J. Cosmol. Astropart. Phys. 06 (2015) 014.
[126] F. Fritsch and R. Carlson, SIAM J. Numer. Anal. **17**, 238 (1980).
[127] F. Fritsch and J. Butland, SIAM J. Sci. Comput. **5**, 300 (1984).
[128] P. A. R. Ade *et al.* (Planck Collaboration), arXiv:1502.01589.
[129] T. Kitayama and Y. Suto, Mon. Not. R. Astron. Soc. **280**, 638 (1996).
[130] B. Sartoris, A. Biviano, C. Fedeli, J. G. Bartlett, S. Borgani, M. Costanzi, C. Giocoli, and L. Moscardini *et al.*, arXiv:1505.02165.
[131] M. Levi *et al.* (DESI Collaboration), arXiv:1308.0847.
[132] M. Tegmark, A. Taylor, and A. Heavens, Astrophys. J. **480**, 22 (1997).

[133] G. Jungman, M. Kamionkowski, A. Kosowsky, and D. N. Spergel, Phys. Rev. D **54**, 1332 (1996).
[134] R. A. Fisher, Ann. Eugen. **6**, 391 (1935).
[135] H. J. Seo and D. J. Eisenstein, Astrophys. J. **598**, 720 (2003).
[136] A. Font-Ribera, P. McDonald, N. Mostek, B. A. Reid, H. J. Seo, and A. Slosar, J. Cosmol. Astropart. Phys. 05 (2014) 023.
[137] L. R. Abramo and K. E. Leonard, Mon. Not. R. Astron. Soc. **432**, 318 (2013).
[138] A. F. Heavens, T. D. Kitching, and L. Verde, Mon. Not. R. Astron. Soc. **380**, 1029 (2007).
[139] P. A. R. Ade *et al.* (Planck Collaboration), Astron. Astrophys. **571**, A16 (2014).
[140] J. M. Maldacena, J. High Energy Phys. 05 (2003) 013.